In-situ high resolution photoelectron spectroscopy study on interaction of sodium with UO2+x film ($0 \leq x \leq 1$)

Concettina Andrello, T. Gouder, Loïc Favergeon, Lionel Desgranges, E. Tereshina-Chitrova, L. Havela, R.J.M. Konings, R. Eloirdi

In-situ high resolution photoelectron spectroscopy study on interaction of sodium with UO_{2+x} film ($0 \leq x \leq 1$)

C. Andrello[a,b,c], T. Gouder[b], L. Favergeon[a], L. Desgranges[c], E. Tereshina-Chitrova[d,e], L. Havela[e], R.J.M. Konings[b], R. Eloirdi[b]

a *Mines Saint-Etienne, Univ. Lyon, CNRS, UMR 5307 LGF, Centre SPIN, Saint-Etienne F-42023, France*
b *European Commission, Joint Research Centre, P.O. Box 2340, Karlsruhe D-76125, Germany*
c *Commissariat à l'énergie atomique et aux énergies alternatives, DEN/DEC/SA3E/LAMIR, Centre de Cadarache, Saint-Paul lez Durance 13108, France*
d *Institute of Physics, ASCR, Prague, Czech Republic*
e *Faculty of Mathematics and Physics, Charles University, Prague 12116, Czech Republic*

Abstract

We studied in-situ the interaction of sodium metal with UO_{2+x} ($0 \leq x \leq 1$) using thin films prepared by sputter deposition on Au substrate. X-ray Photoelectron Spectroscopy (XPS) and Grazing Incidence XRay Diffraction (GIXRD) characterized films before and after interaction. The results show that sodium does not reduce stoichiometric UO_2 at room temperature. Plasmon loss peaks, observed at the Na*1s* photoemission (PE) line, are characteristic of metallic sodium particles, and point to a weak interaction between sodium and UO_2. The oxidation of the sodium at room temperature takes place only on hyperstoichiometric uranium dioxide films. Indeed, sodium deposition on UO_{2+x} ($0 < x \leq 1$), eventually results in the complete reduction of U(VI) down to U(IV). Molecular and atomic oxygen affect differently the oxidation of uranium and sodium. The wetting of the gold by the sodium is much more important when sodium is oxidised by atomic oxygen. This leads to a shift of the Na*1s* core level peak, while molecular oxygen gives a peak broadening without shift. Atomic oxygen seems to play the same role as the interstitial oxygen present in the UO_{2+x} film. The oxygen dissociation may be the limiting step of sodium oxidation on gold and on UO_2. Heat treatment of sodium on UO_3 at about 773 K leads to the formation of the $NaUO_3$ film as demonstrated by a quantitative analysis by XPS and GIXRD. The results show also that once U(V) is formed, it stays stable up to at least 973 K, the temperature at which shrinkage of the film is observed.

1. Introduction

In response to the difficulties in achieving sustainability, with sufficient high degree of safety and more competitive economic bases of nuclear power plants, Generation IV reactors have been considered and amongst selected options, Sodium cooled Fast Reactor (SFR) possesses one of the most attractive designs [1]. The Fukushima Daiichi Nuclear Power Plant accident reemphasized importance of the safety approach in the design of new nuclear reactors to avoid risks related to accidents. To comply with high safety standards, SFRs of Generation IV foresee implementation of an internal storage of spent and failed fuel pins, thus omitting the need of an external sodium pool to avoid potential risks of interaction with air and water. In addition, the SFR design also has the advantage of becoming more compact, reducing a construction cost. Fuel pins with breached clad will be removed from the active core and moved to an internal storage. In-vessel storage of failed fuel pins necessarily leads to a direct contact between the primary coolant and fuel. The reaction product of the interaction between sodium and oxide fuel is generally denoted as Na_3MO_4 (where $M = U$, Pu) [2], characterized by very unfavourable physical properties [3], which might result in fuel pulverization, with the consequence of

radioisotopes dissemination into the primary system. Understanding of the corrosion mechanism becomes then of prime importance for establishing feasibility of an internal storage of failed fuel pins, and may impose strict limits on their management.

Due to complexity of potential phenomena involved in the reactions of real fuel, we first focused on the UO_2 corrosion behaviour. Since the interaction between sodium and fuel starts at the surface, we use thin films in this study to explore the details of such a process. From the thermodynamic point of view, stoichiometric UO_2 should be in equilibrium with pure sodium [4] and consequently it is not expected to react with it. However, changes in the U/O ratio or oxygen content in sodium lead to the formation of a ternary compound. The Na-U-O system contains a wide range of sodium uranium oxides, as reported in Fig. 1, such as Na_3UO_4, Na_4UO_5, Na_2UO_4, $Na_2U_2O_7$, $Na_6U_7O_{24}$, $NaUO_3$. The interaction between hypostochiometric UO_2 and liquid sodium is reported to be different from the one of stoichiometric UO_2 interacting with liquid sodium containing dissolved oxygen [5,6]. At temperatures below 673 K, cracks appear when Na is in contact with a UO_{2+x} pellet [5], probably due to the formation of a sodium monoxide (Na_2O) within grain boundaries [5,6]. However, during the interaction of UO_2 with liquid sodium containing dissolved oxygen, an incoherent surface layer is formed [5]. In the present thin film study, we want to prove reproducibility of these phenomena and explain their origin. Also we know that dissolution of a fuel matrix in the environment is related to uranium oxidation states [7]. Recently, Smith et al. [8] reported that, even with the low O concentration dissolved in liquid sodium, oxidation to U^{6+} may be possible. In the present study, under ultra-high vacuum (UHV) we want to understand the interaction of metallic sodium with uranium oxides, if Na enables to stabilize U(V) or U(VI) oxidation state.

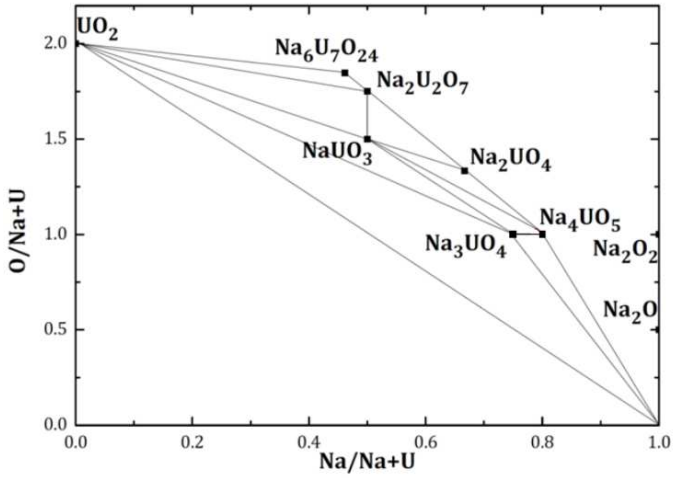

Figure 1. Sodium-uranium-oxygen phase diagram [8]

The present X-ray Photoelectron Spectroscopy (XPS) study is first of a kind dealing with the interaction of metallic sodium with UO_{2+x} ($0 \leq x \leq 1$) using thin films as a surface model. To the best of our knowledge, a very few XPS results on pure metallic and oxide sodium are reported in literature [9,10]. Hence, we first had to establish properties of metallic sodium on a gold substrate as a reference, before to explore the interaction of sodium and UO_{2+x} film. Several questions will be addressed in this study, amongst them the potential of metallic sodium to reduce UO_{2+x} ($0 \leq x \leq 1$). Also we want to elucidate whether the presence of sodium can stabilize uranium in its pentavalent state. We expect for instance to reduce UO_3 into UO_2 by using ultra-high vacuum and heat treatment above a threshold temperature (between ≥400 °C and 500 °C), but what will happen to UO_3 if we include metallic sodium into the

system? Would it be possible to produce in-situ $NaUO_3$ films, and extend our knowledge on its electronic structure?

2. Experimental

2.1. Materials and methods

Thin films of uranium oxide UO_{2+x} ($0 \leq x \leq 1$) are prepared in-situ by a direct current (DC) reactive sputtering from a uranium metal target in a gas mixture of Ar (6 N) and O_2 (6 N). The uranium target voltage is fixed at -700 V. Thin films are deposited for 100 up to 300 s at room temperature on polycrystalline Au substrates. The Au substrates are first cleaned by Ar ion sputtering (3 keV) for 5 min, and subsequently annealed at 573 K for 5 min. The plasma in the diode source is maintained by injection of electrons of 25–50 eV energy (triode setup), allowing working at low Ar pressure in absence of stabilizing magnetic fields. The thickness of the UO_2 overlayer film is estimated by comparing the intensity of the Au*4f* (substrate) and U*4f* (overlayer) photoemission lines. We assume a continuous overlayer, without interdiffusion or extended island formation and an inelastic mean free path of about 1.79 nm and 2.14 nm for U*4f* and Au*4f* lines, in the UO_2 overlayer respectively [10]. We obtain an overlayer thickness of approximately 7 nm for the standard deposition times (100 secs) used in this study. UO_3 films are produced in the atomic chamber by further oxidation of UO_{2+x} films with atomic oxygen, produced by an electron cyclotron resonance (ECR) Plasma Source Gen I from Tectra GmbH, Frankfurt/M. The atom flux is specified to $>10^{16}$ atoms/(cm^2.s), corresponding to an exposure of roughly 10 Langmuir/s (i.e. 10^{-3} Pa O). Preparation and stabilization of stoichiometric UO_2 is obtained by reducing UO_{2+x} with atomic hydrogen produced in the same ECR source, using H_2 (6 N) gas. The heating of the sample is made by e-beam with the thermocouple pressed onto the sample surface. Molecular oxygen was introduced via a leak valve and via a capillary directing oxygen onto the sample surface. Adsorption was performed at 10^{-7} to 10^{-6} mbar oxygen pressure. Oxygen dose was measured in Langmuirs (pressure x time), where 1 Langmuir (L) corresponds to 1.33 10^{-6}mbar $*$ 1 s), which is the dose needed to cover the surface by one monolayer of the adsorbate, if all gas molecules stick on the surface. Sodium layers are prepared by evaporation. The metallic Na (ALDRICH,99.9%) product was carefully cleaned with Hexane (SIGMA ALDRICH, 95%) to remove the mineral oil, in which sodium is stored, and cut in small pieces to be mounted in the electronbeam crucible. The chamber is pumped down rapidly to remove the residual moisture bound to sodium. Then the evaporator is gently heated to 393 K under ultra-high vacuum (UHV) and kept at that temperature for several hours. After 24 h of chamber baking, the electron-beam is switched on and the crucible is further heated starting with 1 W heating power. For evaporation, we use the EFM3 electron beam evaporator from FOCUS. The sodium is placed in a tungsten crucible of 250 mm^3 and a heating power of 15 W is applied. We work at an acceleration voltage of 1 kV, with a sample/crucible distance of 200 mm. The beam intensity is measured by the ion current (ionization of Na atoms by the heating electrons), and a total evaporation amount of 10 mA s (flux time) is chosen. The constant flux time value ensures a constant total amount of Na, because the ion flux/total atom flux ratio can be expected to be constant. The sample-source distance was fixed to 10 cm. Under these conditions, reproducible layer thicknesses were obtained. The thickness was determined by the attenuation of substrate signal (the Au*4f* or U*4f*) or by the overlayer/substate signal ratio (typically Na*1s*/Au*4f* and Na*1s*/U*4f*). Since these values also depend on the mode of growth (wetting), the thicknesses thus indicated are only approximate. For that reason it was even more important to impose strict deposition doses (by the flux time) to ensure constant overlayer thickness.

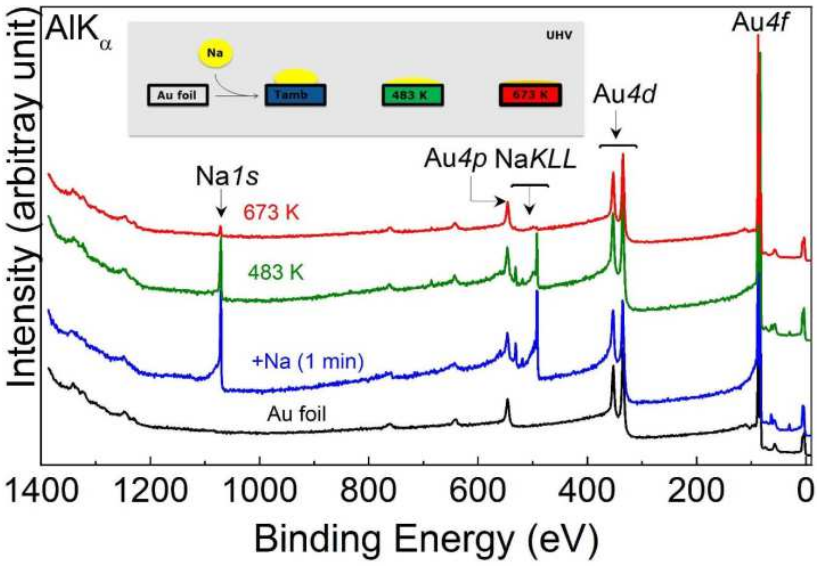

Figure 2. Overview spectra of Au foil (black curve), after Na deposition (blue curve), heat treated at 483 K (green curve) and at 673 K (red curve).

2.2. Characterization

High resolution X-ray photoelectron spectroscopy (XPS) measurements are performed using a Phoibos 150 hemispherical analyser. Al-K$_\alpha$ (E = 1486.6 eV) radiation is produced by an XRC-1000 micro-focus source, equipped with a monochromator and operating at 120 W. The background pressure in the analysis chamber is 2×10^{-10} mbar. The spectrometer is calibrated by using an Au-*4f*7/2 line of metal to give a value at 83.9 eV BE and a Cu-*2*p3/2 line of metal at 932.7 eV BE for XPS. Photoemission spectra are taken at room temperature. Data analysis was performed using CasaXPS software version 2.3.20rev1.2 G. As Relative Sensitivity Factors, Scofield cross-sections for an Al-K*α* radiation [11] were taken. The grazing incidence x-ray diffraction (GIXRD) measurements are done on a Rigaku SmartLab diffractometer usinga 9 kW copper rotating anode x-ray source (Cu-K*α* radiation λ = 0.15418 nm). It is equipped with a parabolic multilayer mirror in the primary beam, a set of axial divergence eliminating soller slits in both the incident and diffracted beam (acceptance 5°) and a parallel beam soller slit collimator (acceptance 0.5°). A HyPix-3000 2D hybrid pixel single photon-counting detector is located in the diffracted beam. The constant incidence angle of the primary beam ω = 1.0° is used for the measurement.

3. Results

3.1. Na deposition on au foil

A gold foil is used as a reference for the interaction of sodium with the UO_{2+x} films ($0 \leq x \leq 1$). Fig. 2 summarizes the results for the deposition of sodium on a gold foil and the effect of temperature. A representative spectrum is reported for each temperature and the process is summarized in the inset. Surface cleanliness of the gold foil (black spectrum) is shown by the absence of carbon and oxygen *1s* peaks at 284.5 eV and 530 eV respectively. Dominant peaks of Au appear at about 100 eV and 350 eV, corresponding to Au*4f* and Au*4d* respectively. After deposition of sodium on the substrate at ambient temperature (blue spectrum), additional peaks at 1072 eV and 425 eV are associated to Na*1s* and Na*2s* respectively. When the substrate is heated at 483 K (green spectrum) and at 673 K (red spectrum),

sodium gradually evaporates, as shown by the intensity decrease of Na photoemission lines. Fig. 3 displays the Na*1s* and Au*4f* core-level spectra obtained after Na deposition and heat treatment with reference to a gold foil. After sodium deposition for 1 min at room temperature a film thickness of about 4 nm is reached as shown by the Na*1s*/Au*4f* intensity ratio. The Na*1s* peak is asymmetric, characteristic of metallic sodium [10,12], with a binding energy (BE) of 1071.2 eV. After the annealing at 483 K, the Na*1s* intensity decreases while the Au*4f* core-level peaks are enhanced and recover almost to their initial intensity at T = 673 K. A slight interdiffusion between sodium and gold at this temperature may explain the presence of a weak Na*1s* intensity peak: It could be attributed to a near surface alloy formed by Na-Au interdiffusion and stable at T = 673 K [13]. We cannot exclude the presence of electronegative element as fluor or oxygen present at trace level and for which the Auger peak peaks are below detection limit. To understand the role of the interstitial oxygen present in the UO_{2+x} films ($0 < x \leq 1$) in the interaction with sodium, it is interesting to look at the reaction of atomic and molecular oxygen with sodium. The question, to be addressed, is the potential catalytic effect of Na on the dissociation of molecular oxygen.

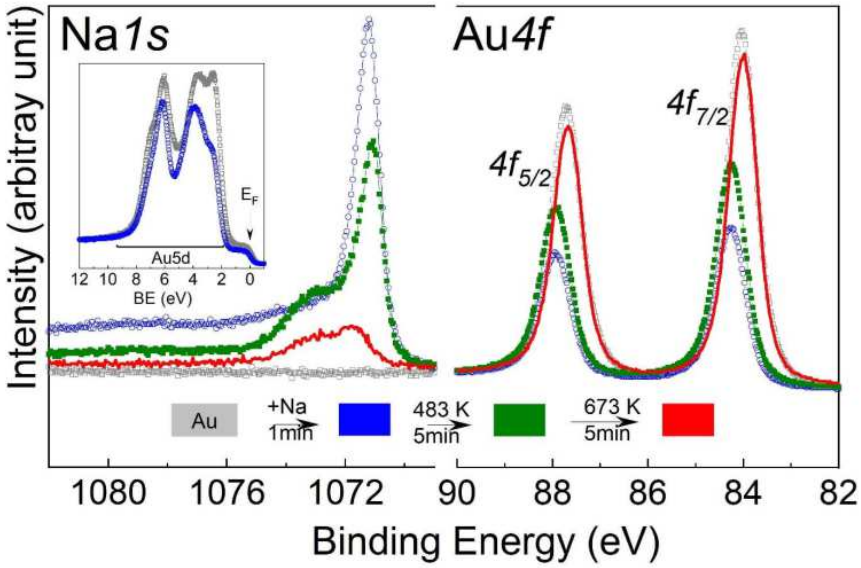

Figure 3. Na-*1s* and Au-*4f* core level spectra obtained on a Au foil (grey curve), after deposition of sodium (blue curve), and heat treatment at 483 (green curve) and 673 K (red curve). Inset: Valence band of Au foil (grey) and of Na deposited on gold (blue).

Fig. 4 (left) reports Na*1s* and Au-*4f*7/2 (inset) core-level spectra after deposition of sodium, followed by a heat treatment at 463 K and oxidation with molecular oxygen. We proceed to the heat treatment at 463 K to favour the diffusion of molecular oxygen into sodium. Fig. 4 (right) reports the same series but using atomic oxygen at ambient temperature instead. The oxidation with molecular oxygen leads to a broadening and higher symmetry of the Na*1s* peak, its BE remaining invariable at ~ 1071.1 eV (BE = -0.2 eV). On the other hand, oxidation with atomic oxygen leads to a symmetric peak shifted to 1073.2 eV (BE = +1.8 eV). This indicates that the oxidation of Na is more important and faster in the presence of atomic oxygen, and in particular that the dissociation of O_2 is the limiting step for oxidation of sodium. Solubility for oxygen in liquid sodium is known and depends largely on temperature [14]. For instance, the oxygen solubility at 773 K (1200 ppm) is 100-times higher than the solubility at 473 K (12 ppm) [15]. A study on sodium adsorbed on MgO [16] assigned the Na*1s* line at about 1072.2 eV to the Na_2O formation. Others [17,10] found the core level peak Na*1s* of Na_2O at 1073.01 eV in agreement with the present study. amongst the sodium oxide compounds reported in literature, there are sodium

monoxide (Na_2O, white solid), sodium peroxide (Na_2O_2, white to yellow solid), sodium superoxide (NaO_2, yellow-orange, metastable at standard condition) and sodium trioxide (NaO_3) [18]. It is confirmed that sodium oxides consist mainly of sodium peroxide and sodium monoxide. From the standpoint of thermodynamics, sodium peroxide is formed when the oxygen fraction is sufficiently large, and sodium monoxide is formed under a relatively low oxygen fraction [19].

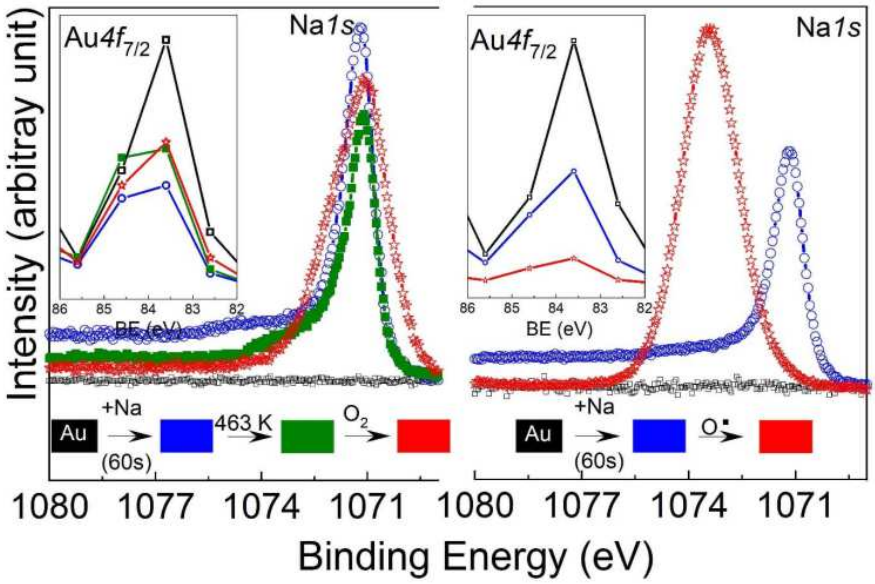

Figure 4. Oxidation study of sodium with molecular and atomic oxygen. Inset: Corresponding variations of the Au-*4f*7/2 peak.

When sodium is heated in air at 403–673 K, it produces Na_2O_2, a process that goes though the generation of Na_2O:

$$4Na + O_2 \rightarrow 2Na_2O$$

$$2Na_2O + O_2 \rightarrow 2Na_2O_2$$

Upon heating above 927 K, Na_2O_2 decompose to Na_2O and O_2.

$$2Na_2O_2 \rightarrow 2Na_2O + O_2$$

$$6Na + 2O_2 \rightarrow 2Na_2O + Na_2O_2$$

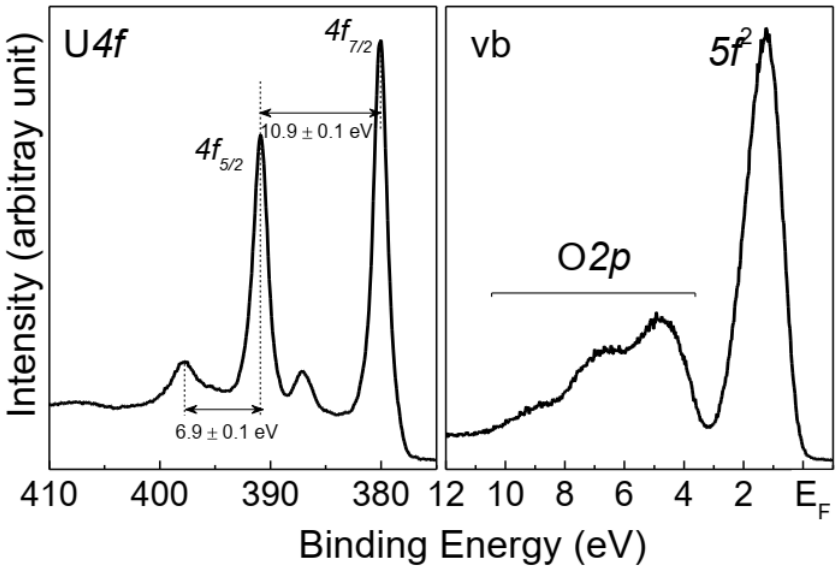

Figure 5. U-4*f* and valence band (vb) of stoichiometric UO_2, obtained after reduction and stabilization of UO_{2+x} by atomic hydrogen at 673 K.

The melting temperatures of Na_2O and Na_2O_2 are 1405 K and 825 K, respectively. The most stable bulk is Na_2O_2 in an oxygen environment at standard conditions [20]. With a higher BE, oxidation of sodium is more efficient in the presence of atomic oxygen compared to sodium in the presence of molecular oxygen. Differences in the Au-*4f*7/2 intensity for different oxidation reactions (molecular versus atomic oxygen) can be linked to the level of coverage of the gold foil. It is becoming more important after oxidation of sodium with atomic oxygen. This can be explained by stronger interaction of the gold surface with sodium oxide than with sodium metal [10]. Once sodium is oxidized, it spreads and covers more the surface of gold. We see that with molecular oxygen, the coverage of gold foil is less effective after the heat treatment and improves slightly after oxidation. It looks like sodium is slightly oxidized, the molecular oxygen is dissolved in sodium, and volume increases at the extent of the surface coverage. After reaction with molecular oxygen, the sodium Na*1s* PE line has BE similar to metallic Na, and the broadening of Na*1s* core level peak may support a partial oxidation.

3.2. Na deposition on UO_2

Further, the potential reaction of sodium on stoichiometric UO_2 film is investigated. To ensure stoichiometry of the films, UO_2 is produced in two steps. An initial oxide film is deposited in the preparation chamber. It is slightly hyperstoichiometric. In the second step it is reduced by exposure to atomic hydrogen for 600 s, keeping the substrate at T = 673 K. This allows stabilizing the uranium oxide as stoichiometric UO_2 since all surplus oxygen reacts with atomic hydrogen. Fig. 5 displays the U4*f* peaks of stoichiometric UO_2. Amongst the indicators are first the satellite peaks at 6.9 eV higher BE than the spin-orbit split (by 10.9 eV) 4*f*5/2 and 4*f*7/2 main peaks [21,22]. Also the corresponding valence-band spectrum displays the *5f*2 peak at about 1.3 eV and the O*2p* states, with a peak intensity ratio characteristic of UO_2 [22]. The absence of peak at 10 eV, characteristic of OH group, support the absence of hydrogen on the film. Also the symmetry of O*1s* peak reported in Fig. 6 (middle, black spectrum) comforts the absence of OH group in the sample. Stoichiometric UO_2 is obtained through reduction with atomic hydrogen while sample is kept at 673 K, temperature at which water is desorbed from the surface of the film. Fig. 6 shows the normalized U*4f*, O*1s*, Na*1s*, and valence-band spectra after deposition of about 2 nm Na on UO_2 at room temperature (blue spectra) compared with a clean

UO_2 film (black spectra). Metallic sodium is visible as shown by the plasmon loss peaks at E = 5.8 eV in the Na*1s* spectrum, which is in good agreement with literature [23]. The U*4f* peaks shift to slightly higher binding energy (black to blue spectrum). The higher background is due to the inelastic scattering of U*4f* photoelectrons, showing uranium underneath the Na overlayer. The satellite peak position stays constant at 6.9 eV higher BE than the main line. This "6.9 eV satellite" is an indication for U(IV) present in UO_2 form [24,25]. This is also supported by the similar valence band (inset Fig. 6, black and blue spectra) keeping the same intensity ratio of O*2p*/*5f* [21], with a slight shift induced by the sodium overlayer. The O*1s* spectra obtained after deposition of Na undergo a slight shift to higher binding energy and a second peak appears at about 537 eV. This later can be related to the Na-*KLL* emission or to physisorbed Na on the oxide. This experiment allows us to conclude that Na reduces the stoichiometric UO_2 neither at room temperature nor at T = 463 K (not shown here).

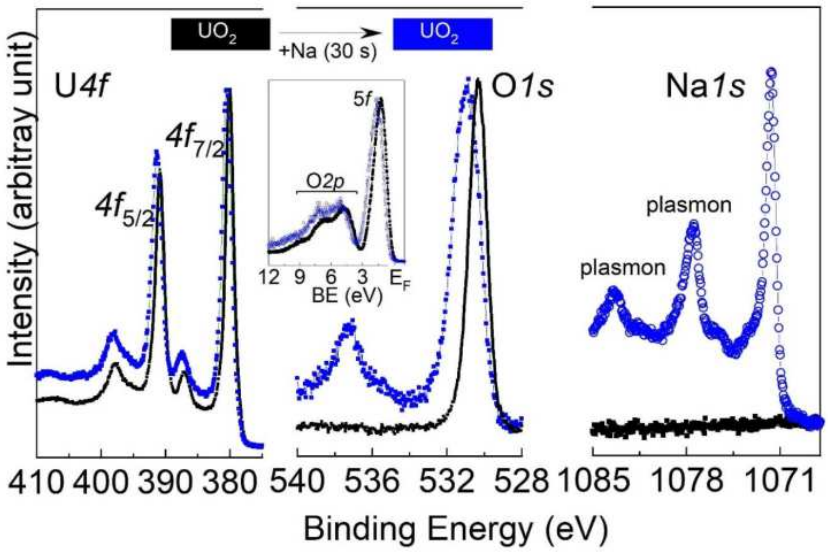

Figure 6. Effect of Na deposition on UO_2 before and after heat treatment at 463 K observed in U-*4f* (left), O-*1s* (middle), and Na-*1s* (right) spectra. The inset displays the valence band spectra.

3.3. Na deposition on UO_{2+x} ($0 < x \leq 1$) film at ambient temperature

The next question is about possible reduction of UO_{2+x} by metallic Na. Fig. 7 describes two successive depositions of sodium on UO_3 and one deposition on UO_{2+x}, both at room temperature. The corresponding O*1s* and U*4f* core-level spectra are reported for each step of the experiment. Following the position of the satellite peaks, we can determine the oxidation state of uranium. The result demonstrates that metallic sodium reduces UO_3 into UO_2 at room temperature. The two satellite peak, satVI, characteristic of UO_3 [21] (black spectrum) disappear at the extent of a single satellite peak, satIV, characteristic of UO_2 (green spectrum). Also the U-*4f*7/2 BE shift to lower BE can be linked to the reduction process of UO_3 into UO_2, although for this latter, corresponding U-*4f*7/2 BE at 380.6 eV is shifted compared to clean UO_2 at 380 eV reported in Fig. 6 (black spectrum). Also, for UO_2, we expect one single peak for O*1s* as reported in Fig. 6 (middle, black spectrum), with a BE at 530.3 eV. Fig. 7 shows that successive deposition of metallic sodium on initial UO3 sample (black spectrum) goes from O*1s* spectrum with two peaks (blue spectrum), 530.4 eV and 535.5 eV to one peak (green spectrum) whose BE is at 530.7 eV shifted also from BE of O*1s* present in clean UO_2 (Fig. 6, black spectrum). The corresponding Na*1s* line obtained on UO_{2+x} ($0 < x \leq 1$), appears as a single and symmetric peak characteristic of oxidized sodium. The interstitial oxygen present in UO_{2+x} seems to play the same role as atomic oxygen does in the oxidation of sodium.

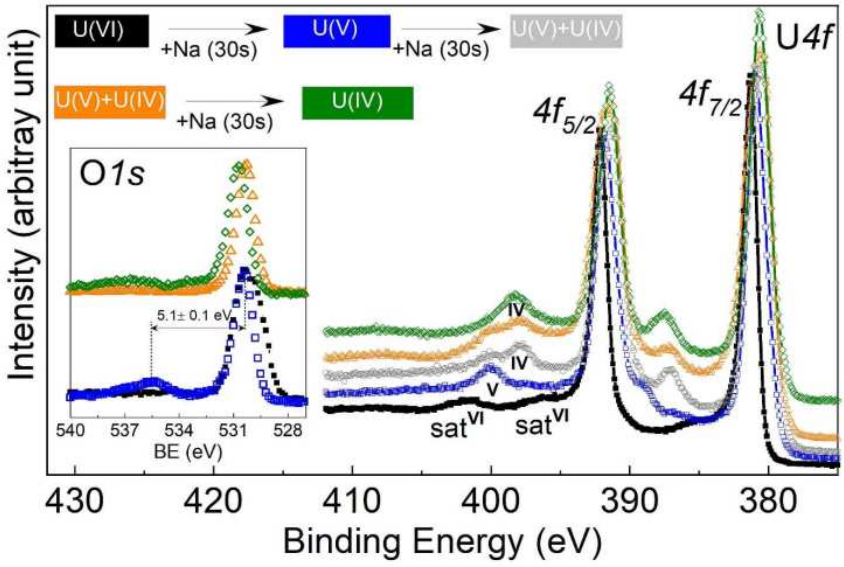

Figure 7. U-*4f* and O-*1s* core-level spectra before and after successive deposition of Na on UO_3 and UO_{2+x} at room temperature.

Fig. 8 compares the Na*1s* spectra obtained on Au after oxidation with molecular and atomic oxygen (orange, blue and gray spectra), on stoichiometric UO_2 without without and with molecular oxygen (green and red spectra) and on UO_{2+x} (black spectrum). Na stays metallic on Au and UO_2. While for UO_2 we observed plasmon peaks, on Au we do observe only single and asymmetric peak. The difference could be explained by the shape of sodium deposit at the surface of samples. As sodium has a higher wettability on gold [26], deposition leads to a growth along the layer while on UO_2 it rather forms 3D particles. Oxidation of sodium requires either a deposition on UO_{2+x} (black spectrum) or oxidation with atomic oxygen on gold foil (grey spectrum). In both cases, the Na*1s* peak is at about 1073 eV BE versus 1071.5 eV for metallic Na. An intermediate case between oxide and metallic sodium appears when oxidation is performed with molecular oxygen on gold (blue spectrum) and on the UO_2 film (red spectrum). The corresponding BE between 1071 and 1071.8 eV, respectively, is close to the one of metallic sodium and ternary compounds, such as $NaUO_3$. Based on the experiment represented in Fig. 4, we can deduce that the oxidation of sodium is taking place directly with interstitial oxygen present in UO_{2+x}. On stoichiometric UO_2, Na does not seem to oxidize under our experimental conditions and the dissociation of molecular oxygen seems to be the limiting step for oxidizing sodium. This is also supported by the fact that UO_2 oxidizes into UO_{2+x} with molecular oxygen. Poor wetting is due to a weak interface interaction between non-reactive metalliono-covalent oxides. It is not strong enough to counterbalance the metallic bond in the neighbourhood of the interface [27]. To increase wettability of oxides by liquid metals, dissolution of oxygen even on the ppm level [14] is necessary. This phenomenon, explained by Naidich et al. [28], suggests that oxygen, dissolved in the metal, associates with metal atoms and forms clusters having a partially ionic character, with a charge transfer from the metal to the oxygen atoms. These clusters can develop Coulomb interactions with ionocovalent ceramics and, consequently, adsorb strongly to the metal/oxide interfaces. Compared to the Na*1s* BE of metallic sodium at 1071.5, the 0.7 eV higher BE in Na/UO_2 plus O_2 match the difference between Na_2O and metallic Na [16,10], suggesting that the Na oxidizes together with UO_2 in presence of molecular oxygen resulting in the formation of an oxidic sodium compound [29]. Na*1s* in ternary compounds has a BE of 1071.8 eV, close to the one of metallic Na, but it is broader than Na*1s* present in metallic.

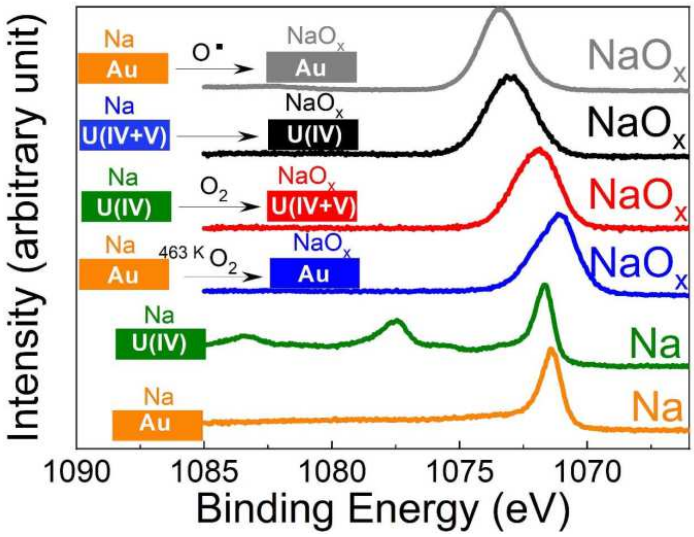

Figure 8. Na-*1s* core-level spectra obtained after deposition on Au foil (orange curve), on UO_2, on UO_{2+x} and on UO_2 followed by oxidation with molecular or atomic oxygen.

4. Na deposition on UO_3 film versus temperature

$NaUO_3$ and Na_3UO_4 are the only two sodium uranate compounds with the U(V) oxidation state. While Na_3UO_4 structure has been assigned recently as monoclinic (space group P2/c) [8], $NaUO_3$ with an orthorhombic perovskite structure (space group *Pbnm*) has been an object of investigation over many years [30]. To establish if this compound could be formed under our experimental conditions and studied in-situ, we focused on an effect of temperature when Na is deposited on the UO_3 film. Fig. 9 displays the U*4f*, O*1s*, Na*1s* spectra at various temperatures. It is insightful to compare the satellites in the 4*f* spectra plotted as a function of relative energy difference to the main peak, BE. At room temperature, Na reduces UO_3 into UO_{2+x} with mixed U(V) and U(IV). At 523 K, U(V) becomes the major oxidation state in the sample.

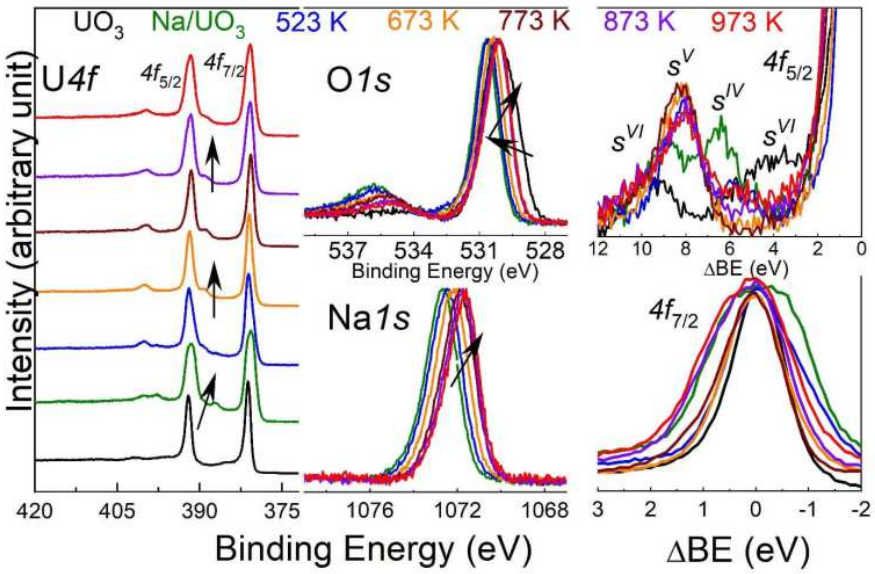

Figure 9. Effect of temperature on Na/UO_3 followed on U-*4f*, O-*1s*, and Na-*1s* spectra. Right top, details of satellite peaks plotted as a function of ΔBE related to the main 4*f* peak. The black arrows indicate the shifts with increasing temperature.

Then from 673 K till 873 K, U(V) is the single oxidation state. Relating the spectra to BE we can easily compare the broadening of the peaks as a function of temperature. Without considering the UO_3 spectrum, the smallest broadening is observed at 673 K and 773 K, which points to a single phase (or oxidation state) formed at these temperatures. The largest broadening is obtained at room temperature for sodium deposited on UO_3, corresponding to a heterogeneous system. The O*1s* spectrum shows a shift of the main peak in two steps (black arrow), first to higher BE and then from 523 K it goes to lower BE. A second peak appears at 5 eV higher BE from the main peak. Na*1s* shows one single and symmetric peak, being representative of oxidized sodium, all along the experiment. It shifts monotonously to lower BE from 1072.6 to 1071.6 eV. To support the formation of a ternary compound between uranium trioxide and sodium at 673 K –773 K, a XPS study was taking place with heat treatment of uranium trioxide under UHV conditions (Fig. 10).

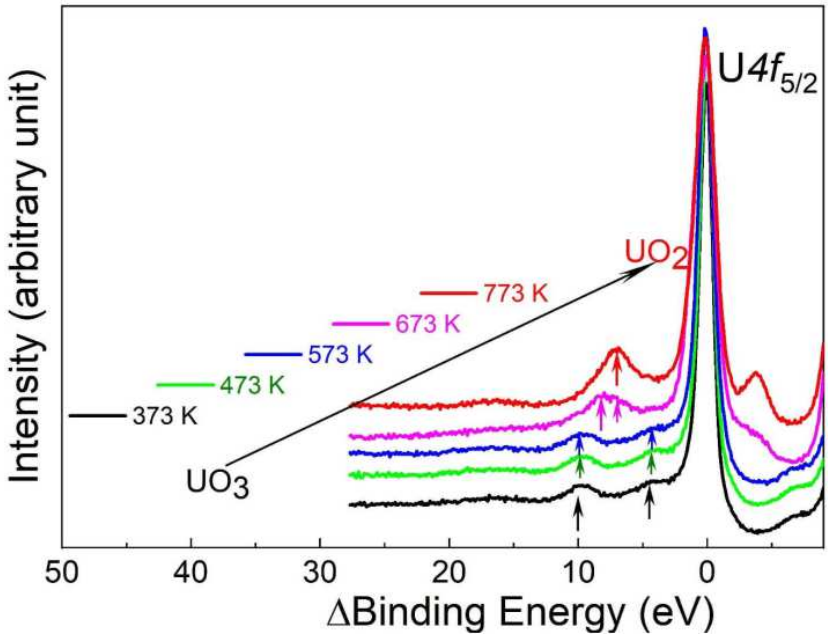

Figure 10. U*4f* core level spectra along heat treatment under ultra-high vacuum

All the U-*4f*7/2 have been set at the same BE to compare more easily the relative position of the satellite peaks [21]. The result shows that when the temperature reaches 773 K the UO_3 film (black spectrum), characterised by its BE (U-*4f*7/2 _ 381.5 eV) and the two satellites peaks at 4 and 10 eV, reduces to a close composition of UO_2 (red spectrum) characterised by it's BE (U-*4f*7/2 _ 380.5 eV versus 380.0 eV for pure UO_2, Fig. 5) and by a satellite peak at 6.9 eV. In between at 678 K, we observe the appearance of the "8 eV" (pink spectrum) which is linked to the intermediate oxidation state U(V). Fig. 10 associated to Fig. 7, with reduction of UO_3 by Na at room temperature, enable to argue that the combination of Na on UO_3 with a heat treatment to 673–773 K may lead to the formation of a ternary compound with stabilized pentavalent uranium. Corresponding valence band spectra of the films obtained by reaction of sodium with UO_3 at various temperatures are shown in Fig. 11 (left). Following the evolution of the 5*f* peak between 2 and 1 eV, Na reduces uranium in UO_3 (black spectrum), in which the 5*f* peak is absent. To better follow the shift and the FWHM of the 5*f* peak reported in Fig. 11 (left), related values are plotted as a function of temperature in Fig. 11 (right). The 5*f* states (and their FWHM) shift down till 773 K, from 1.9 eV (1.3 eV) to 1.5 eV (1.0 eV). Then the trend of energy shift changes

while FWHM starts to increase up to 973 K. Based on the Na-U-O ternary phase diagram, pentavalent uranium can be associated either with $NaUO_3$ or Na_3UO_4.

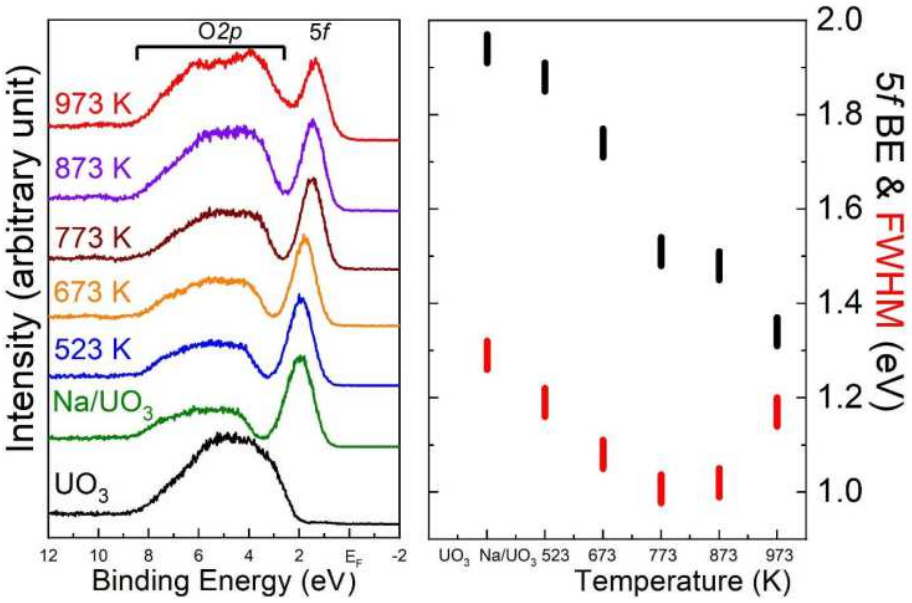

Figure 11. Effect of temperature on Na/UO_3 followed by valence band spectra (left) and energy of the 5*f* peak and its FWHM (right).

Fig. 12 summarises the composition as function of temperature, by following total intensities of the U*4f*, Na*1s*, and O*1s* core-level lines obtained in the overview spectra. From room temperature on, the uranium and oxygen concentrations increase at the expense of Na, which decreases progressively till 973 K. A step in the concentration of O between 673 K and 773 K is observed. A change of slope for both oxygen and uranium seems to take place just above these temperatures. While the oxygen and uranium concentrations appear to be correlated, for Na it is less evident. Based on the overview spectra (not shown here), we can deduce the formation of cracks at 973 K, revealed in appearance of the Au*4f* peaks of the underlying gold foil. The composition obtained at 773 K is within the uncertainty of the XPS technique close to the $NaUO_3$ compound. To obtain additional evidence, we studied the crystal structure of such produced $NaUO_3$ films, starting with a thicker film of UO_3 and using a grazing-incidence x-ray diffraction (see Fig. 12 (right)). The diffraction pattern is compared to known peak positions of $NaUO_3$, PDF2 [01–084–1865] and of the gold substrate. The identified peaks can be indeed assigned mainly to the gold substrate and to $NaUO_3$ mainly. A broad peak at about 28° in 2 can be attributed to amorphous UO_3 or UO_{2+x}. This result corroborates the formation of $NaUO_3$ by the reaction of UO_3 with Na at T = 773 K under UHV conditions.

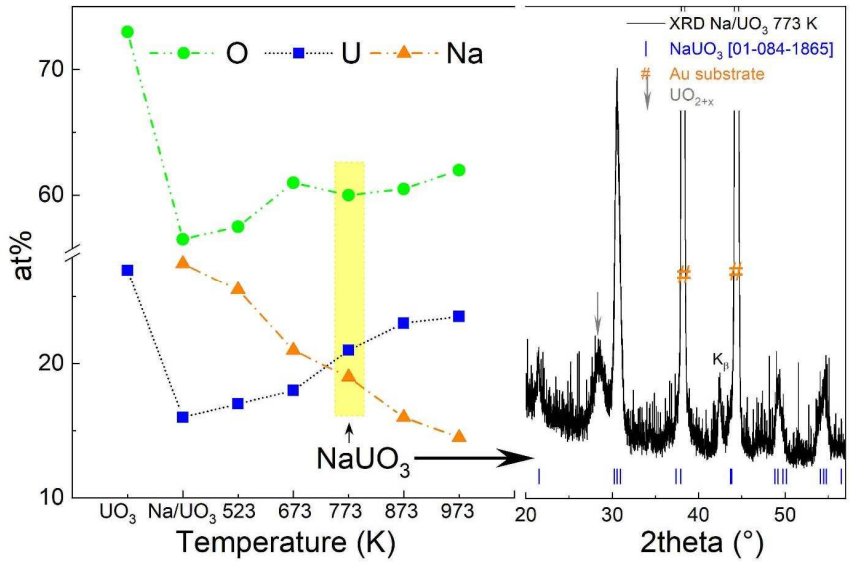

Figure 12. U, Na, and O atomic concentrations as a function of temperature determined by XPS (left). Grazing incidence x-ray diffraction pattern of Na/UO_3 heated at 773 K.

Fig. 13 (left) displays the complete set of U*4f*, O*1s*, Na*1s* corelevel and valence-band spectra of the $NaUO_3$ film produced in-situ. We compare them with those obtained on a U_2O_5 film as reference for U(V) [21]. The "8 eV" satellite peak present in $NaUO_3$ is very well defined. The U-*4f*7/2 and U-*4f*5/2 peaks with respective binding energies of 380.8 eV and 391.5 eV are very similar and slightly narrower comparing to U_2O_5, the same is true for the O*1s* spectrum displays two peaks at 530.1 and 535.2 eV, while the Na*1s* emission exhibits a single peak at 1071.9 eV, which is close to that in metallic Na, but the peak is broader. Besides the additional peak in the O*1s* spectrum, there is a certain difference in the valence-band XPS, which dwells in the proportion of the feature close to the Fermi level *E*F, reflecting the *5f* states, and the broad emission in the range 3–8 eV BE, being mostly due to the O*2p* states. Both spectra have been taken with different constant pass, which may explain the difference, consisting in a small narrowing of the 5*f* feature, FWHM being reduced from 1.15 eV in U_2O_5 to 1 eV.

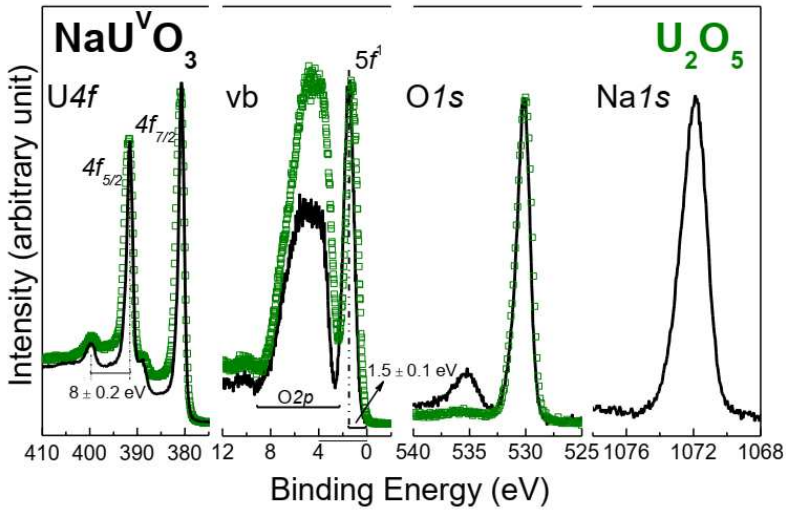

Figure 13. U-4*f*, valence band (vb), O-*1s*, and Na-*1s* core-level spectra observed for $NaUO_3$ film (black) in comparison with U_2O_5 (green) [21].

There is little evidence in literature about XPS on a bulk sample of $NaUO_3$. The U4*f* spectra by Liu et al. [31] are displayed in Fig. 14 together with $Ba_2U_2O_7$ bulk samples and compared to the $NaUO_3$ film obtained in our present study. The binding energies and presence of the satellite peaks are similar. The better resolved "8 eV" satellite peak for the $NaUO_3$ film can be due to the disorder or changes of stoichiometry induced by Ar ion sputtering, used by Liu et al. [31] to clean the surface. On the other hand, in-situ synthesized samples do not require any cleaning. The bulk sample of $Ba_2U_2O_7$ exhibits very similar spectrum, shifted by 0.6 eV towards higher binding energies due to a different chemical environment.

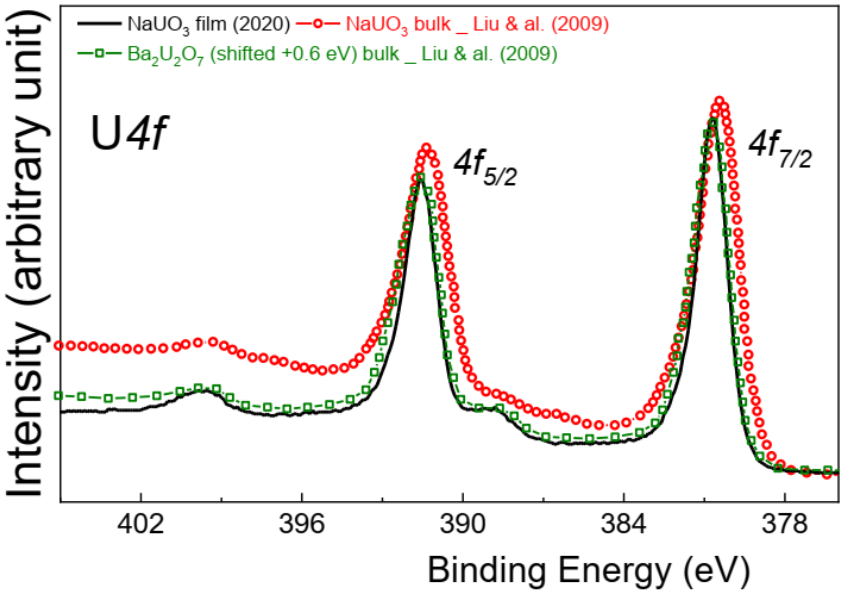

Figure 14. U-*4f* core level spectra of the $NaUO_3$ film, prepared in the present study, compared to the spectra of $NaUO_3$ bulk and $Ba_2U_2O_7$ bulk by Liu et al. [31].

Summary and conclusion

Interaction study of sodium metal with UO_{2+x} ($0 \leq x \leq 1$) thin films is conducted in-situ using XPS and GIXRD as characterization techniques. Deposition of sodium on gold substrate up to 673 K is studied and is to be taken as reference. Molecular and atomic oxygen affect differently the oxidation of sodium on gold and on uranium oxides. Thus wetting of the gold is much more important when sodium is oxidised by atomic oxygen. Atomic oxygen seems to play an identical role as interstitial oxygen present in UO_{2+x}. The oxygen dissociation seems to be the limiting step of sodium oxidation on gold and on UO_2, and the catalytic effect of sodium is weak at temperatures below 473 K. The results demonstrate that Na does not reduce stoichiometric UO_2 at room temperature. The deposition of Na on stoichiometric UO_2 yields plasmon effects of metallic particles formed at the surface. The oxidation of Na at room temperature is observed only on hyper-stoichiometric uranium oxide films, such as UO_{2+x}, as well as UO_3. Deposition of metallic sodium on UO_3 leads to a complete reduction from U(VI) to U(IV). The synthesis of $NaUO_3$ film is possible by heat treatment of Na/UO_3 at about 773 K as confirmed by grazing incidence x-ray diffraction. The results show that once U(V) is formed, it remains stable up to at least 973 K, the temperature at which films start to shrink and crack similar to the crack formation reported in literature for UO_2 pellets. In interaction with UO_3 and above 573 K, sodium stabilizes the formation of pentavalent uranium compounds. In future we intend to follow the interaction of Na with UO_{2+x} ($0 \leq x < 1$) under oxygen flow at higher temperatures to learn whether Na stabilizes rather pentavalent or hexavalent uranium based compounds.

Acknowledgements
E. T.-Ch. acknowledges support of “Nano-materials Centre for Advanced Applications,” Project No. CZ.02.1.01/0.0/0.0/15_003/0000485, financed by ERDF. We want to thank Prof. R. Caciuffo for the numerous suggestion and for fruitful discussion and F. Huber for the technical support.

References
[1] M. Joyce, Chapter 11 - advanced reactors and future concepts, 2018, Pages 263–295, doi:10.1016/B978-0-08-100962-8.00011-1.
[2] H. Kleykamp, Assessment of the physico-chemical proprieties of phases in the Na-U-Pu-O system, KfK4701 (1990).
[3] D.T. Costin, L. Desgranges, T. Retegan, C. Ekberg, Storage of defective fuel pins in SFR core, 5th international ATALANTE conference on nuclear chemestry for sustainable fuel cycles, Procedia Chem. 21 (2016) 378–385.
[4] M.A. Mignanelli, P.E. Potter, The reaction of sodium with urania-ceria solid solutions, J. Nucl. Mater. (1983) 150–185.
[5] M.A. Mignanelli, P.E. Potter, An investigation of the reaction between sodium and hyperstoichiometric urania, J. Nucl. Mater. (1983) 168–180.
[6] M.A. Mignanelli, P.E. Potter, On the chemistry of the reaction between liquid sodium and urania-plutonia fuel for fast breeder nuclear reactors, Thermochim. Acta (1988) 143–160.
[7] D.W. Shoesmith, S. Sunder, W.H. Hocking, Electrochemistry of UO_2 nuclear fuel, in: J. Lipkowski, P.N. Ross (Eds.), Electrochemistry of Novel Materials VCH publishers, New York, 1994.
[8] L. Smith, P.E. Raison, L. Martel, D. Prieur, T. Charpentier, G. Wallez, E. Suard, A.C. Scheinost, C. Hennig, P. Martin, K.O. Kvashnina, A.K. Cheetham, R.J.M. Konings, A new look at the structural proprieties of trisodium uranate Na_3UO_4, Inorg. Chem. (2015) 3552–3561.
[9] S.P. Kowalczyk, L. Ley, F.R. McFeely, R.A. Pollal, D.A. Shirley, The relative effect of extra-atomic relaxation on auger and ESCA shifts in transition metal and salt, PRB (1973).
[10] A. Barrie, F.J. Street, An auger and x-ray photoelectron spectroscopic study of sodium metal and sodium oxide, J. Electron Spectrosc. Relat. Phenom. (1975) 1–31.
[11] N. Fairley, XPS Manual 2.3.15 Introduction to XPS and AES, CASA Software Ltd, 2009, pp. 1–177.
[12] J.F. Moulder, W.F. Stickle, P.E. Sobol, K.D. Bomben, Handbook of X-ray Photoelectron Spectroscopy, 1992.
[13] A.D. Pelton, Bulletin of alloy phase diagrams 1986 (Vol. 7 No. 2) 136-139, “The Au-Na (Gold-sodium) system”.
[14] R.L. Eichelberger, The solubility of oxygen in liquid sodium, AI-AEC- (1968) 12685.
[15] Masahiro Nishimura, Keiichi Nagai, Takamitsu Onojima, Jun-ichi Saito, Kuniaki Ara, Ken-ichiro Sugiyama, J. Nucl. Sci. Technol. 49 (1) (2012) 71–77.
[16] H. Onishi, C. Egawa, T. Aruga, Y. Iwasawa, Adsorption of Na atoms and oxygen-containing molecules on MgO(100) and (111) surfaces, Surf. Sci. 191 (1987) 479–491.
[17] A.P. S.avintsev, Yu O Gavasheli, Z. Kh Kalazhokov, Kh Kh Kalazhokov, J. Phys. Conf. Ser. 774 (2016) 012118.
[18] H.A. Wriedt, The Na-O (sodium-oxygen) system, Bull. Alloy Phase Diagr. 8 (3) (1987) 234–246.
[19] M. Nishimura, K. Nagai, T. Onojima, J.-.I. Saito, K. Ara, K.-.I. Sugiyama, The sodium oxidation reaction and suppression effect of sodium with suspended nanoparticles – growth behavior of dendritic oxide during oxidation, J. Nucl. Sci. Technol. 49 (1) (2012) 71–77.
[20] S. Mohammad, B. Khajehbashi, L. Xu, G. Zhang, S. Tan, Y. Zhao, L.-.S. Wang, J. Li, W. Luo, D.-.L. Peng, L. Mai, Nano Lett 14 (2014) 1016–1020.

[21] T. Gouder, R. Eloirdi, R. Caciuffo, Direct observation of pure pentavalent uranium in U2O5 thin films by high resolution photoemission spectroscopy, Sci. Rep. 8 (2018) 8306.
[22] J.R. Naegele, J. Ghijsen, L.In Manes, L. Manes (Ed.), Actinides - Chemistry and Physical Properties. Structure and Bonding, 59/60, Springer, Berlin, Heidelberg, 1985.
[23] K.D. Tsuei, E.W. Plummer, A. Liebsch, K. Kempa, B. Bakshi, Multipole plasmon modes at a metal surface, Phys. Rev. Lett. 64 (1990) 44.
[24] E.S. Ilton, P.S. Bagus, Ligand feld efects on the multiplet structure of the U4f XPS of UO_2, Surf. Sci. 602 (2008) 1114–1121.
[25] Eugene S. Iltona, Paul S. Bagus, XPS determination of uranium oxidation states, Surf. Interface Anal. 43 (2011) 1549–1560.
[26] J.W. Taylor, S.D. Ford, Solid metal-liquid metal interaction studies, Part II. Contact angle relationships for sodium on solids, 1955.
[27] N. Eustathopoulos, B. Drevet, J. Phys. III France 4 (1994) 1865–1881 https://hal.archives-ouvertes.fr/jpa-00249229.
[28] Yu.V. Naidich, Progress in surface and membrane science 14 (1981) 353–484.
[29] X. Feng, D.F. Cox, Surf. Sci. 645 (2016) 23–29.
[30] A.L. Smith, P.E. Raison, L. Martel, T. Charpentier, I. Farnan, D. Prieur, C. Hennig, A.C. Scheinost, R.J.M. Konings, A.K. Cheetham, A 23Na magic angle spinning nuclear magnetic resonance, XANES, and high-temperature X-ray diffraction study of $NaUO_3$, Na_4UO_5, and $Na_2U_2O_7$, Inorg. Chem. 53 (1) (2014) 375–382.
[31] J.-.H. Liu, S. Van den Berghe, M.J. Konstantinovic, XPS spectra of the U^{5+} compounds KUO_3, $NaUO_3$ and $Ba_2U_2O_7$, J. Solid State Chem. (2009) 1105–1108.